

Including Coriolis effects in the Prandtl model for katabatic flow

Ivana Stiperski,^{a*} Iva Kavčič,^b Branko Grisogono^b and Dale R. Durran^c

^a *Meteorological and Hydrological Service, Croatia*

^b *Department of Geophysics, Faculty of Science, University of Zagreb, Croatia*

^c *Department of Atmospheric Sciences, University of Washington, WA, USA*

ABSTRACT: Katabatic flow down long glaciers in high latitudes experiences deflection due to the Coriolis force. If the Coriolis force is added to the classic Prandtl model for katabatic flow, the cross-slope wind component does not approach a true steady state, but rather diffuses upwards in time. On the other hand, the down-slope component and the potential temperature perturbations do reach stationarity on the same time-scale as in the classic Prandtl model. Numerical and approximate analytic solutions are presented describing this spatio-temporal behaviour. Both solutions are in accordance with physical intuition. The analytic approximate solution can be useful in boundary-layer parameterizations and data analysis. Copyright © 2007 Royal Meteorological Society

KEY WORDS diffusion; polar vortex; steady state; strongly stable boundary layers

Received 11 October 2005; Revised 2 June 2006

1. Introduction

A pure katabatic flow is a relatively shallow but persistent flow that develops in stable atmospheric boundary layers (ABL) on inclined radiatively cooled surfaces, especially over glaciers. It plays an important part in the atmospheric general circulation at high latitudes (Renfrew, 2004) and thus has significant impact on the climate of areas such as Antarctica and Greenland. It is characterized by a pronounced low-level jet and sharp near-surface vertical temperature gradient (Grisogono and Oerlemans, 2001).

One of the simplest models of katabatic flows represents a balance between negative buoyancy production due to the surface potential temperature deficit and dissipation by turbulent fluxes (Egger, 1990). On long glaciers in higher latitudes the Coriolis force also becomes an important contributor to the katabatic flow balance, leading to the occurrence of a wind component directed across the slope. This cross-slope wind component results solely from deflection of the down-slope component by the Coriolis force and is not driven thermodynamically. Measurements (Renfrew, 2004) and numerical simulations (van den Broeke *et al.*, 2002) indicate its considerable strength; furthermore, its vertical scale is larger than the characteristic depth of the down-slope component. An association with the circum-polar vortex on Antarctica has also been suggested (van den Broeke and van

Lipzig, 2003). However, in the observed data and complex numerical models it is very difficult to distinguish between the driving forces, consequent responses, and final effects. Therefore, we use a simple analytic model to discriminate between the different influences and feedbacks.

Parmhed *et al.* (2004) showed agreement between observations of katabatic flows and the Prandtl model. Thus, it is reasonable to extend the Prandtl model so that it includes the Coriolis force in the simplest possible way, to be able to cover long polar slopes and the corresponding long-lived strongly-stable ABL. The latter may have a very large gradient Richardson number over long distances.

Recent research shows large thermal sensitivities of the polar regions to changes in climate forcing (Denby *et al.*, 2002; Heinemann and Klein, 2002), so one should strive more for better parameterizations of strongly-stable polar boundary layers in climate and numerical weather prediction (NWP) models (Derbyshire, 1999; S. Zilitinkevich, personal communication, 2005). In particular, our knowledge on the interactions between turbulence and large-scale geophysical processes remains insufficient. Although a lot of focus has been placed on down-scale influences of large-scale circulations, here we investigate how a phenomenon limited to the boundary layer influences the larger scale, e.g. how strongly-stratified turbulence may impact the large-scale flow. We will tackle this question for a simple, idealized, environment, a long cold slope. Unlike the strongly-stable ABL in flat terrain, where turbulence is not necessarily surface induced, in the ABL on sloping surfaces the katabatic flow jet

* Correspondence to: Ivana Stiperski, Meteorological and Hydrological Service, Grič 3, HR -10000 Zagreb, Croatia.
E-mail: stiperski@cirus.dhz.hr

is the main source of turbulence production (Parmhed *et al.*, 2004). While low-level jets remain one of the central points of mesoscale and ABL interests (Conangla and Cuxart, 2006), we ask ourselves how the inclusion of the Coriolis force and the presence of a cross-slope jet alters this turbulence production and what might its influence be on the dynamics of the katabatic boundary layer and the atmosphere above.

This work extends that of Parmhed *et al.* (2004) and Stiperski *et al.* (2005), who examined asymptotic solutions for katabatic boundary-layer flows. These solutions, as well as the ones proposed here, are needed to explain various measurements, e.g. over the Antarctic, and provide better parameterizations in climate models.

The paper is organized in the following way. In section 2 we derive the set of equations of the rotating Prandtl model, its solutions and note the peculiarities introduced by the Coriolis force. In section 3 numerical solutions and a time-dependent asymptotic solution are presented. The conclusions are given in section 4.

2. Rotating Prandtl model

The classical Prandtl model is, so far, perhaps the best ‘simple’ model available that describes pure katabatic flows (Mahrt, 1982; Egger, 1990; Parmhed *et al.*, 2004). Its simplicity, in that it provides analytic solutions while still retaining all the essentials of the katabatic flow, makes it a suitable tool for studying the influence of different factors on katabatic flows.

We derive the system of equations of the Prandtl model in the following way. Let us consider one dimensional Boussinesq flow parallel to a plane sloping off the horizontal at an angle α (positive counter-clockwise, here negative). Let x be the coordinate pointing down the slope, z be the coordinate perpendicular to the slope, and y the horizontal coordinate parallel to the slope such that (x, y, z) form a right-hand coordinate system. Let (U, V, W) be the velocity vector in these coordinates, where U is the down-slope and V the cross-slope component. After this coordinate transformation, assuming that $W = 0$ at $z = 0$, finite-amplitude disturbances independent of x and y satisfy

$$\frac{\partial U}{\partial t} = g \frac{\theta}{\theta_0} \sin(\alpha) + fV \cos(\alpha) + K \text{Pr} \frac{\partial^2 U}{\partial z^2}, \quad (1)$$

$$\frac{\partial V}{\partial t} = -fU \cos(\alpha) + K \text{Pr} \frac{\partial^2 V}{\partial z^2}, \quad (2)$$

$$\frac{\partial \theta}{\partial t} = -\gamma U \sin(\alpha) + K \frac{\partial^2 \theta}{\partial z^2}. \quad (3)$$

Here θ is the potential temperature perturbation (total minus the background prescribed potential temperature), γ is the constant gradient of the background potential temperature in the true vertical, θ_0 is a reference temperature, and f is the Coriolis parameter. The eddy thermal conductivity K is also assumed constant,

Pr is the constant turbulent Prandtl number and g is acceleration due to gravity. The last terms in Equations (1)–(3) parameterize turbulent fluxes.

No small-amplitude or scaling approximations are required to arrive at (1)–(3), a circumstance that has apparently not been previously noted. Finite-amplitude disturbances that are independent of x and y satisfy Equations (1)–(3) because the advection terms, which would otherwise appear in these equations, are identically zero; as may be verified as follows. Owing to the assumed uniformity with respect to x and y , there is no transport by the slope-parallel velocities; furthermore, the Boussinesq continuity equation reduces to

$$\frac{\partial W}{\partial z} = 0. \quad (4)$$

Since $W = 0$ at $z = 0$, Equation (4) implies that $W = 0$ always, thus the remaining component of the advective transport is also zero. For further details of the derivation see the Appendix.

This system is very similar to that given by Denby (1999), the exception here being a $\cos(\alpha)$ multiplying the Coriolis term in the y momentum equation. For gradually varying $K(z)$ one may use an approach as in Grisogono and Oerlemans (2002), but this is omitted here for simplicity.

If $C < 0$ is the constant surface-potential-temperature deficit, applied to an undisturbed atmosphere–surface interface instantaneously at $t = 0$, the boundary conditions (BC) at the surface for the time-dependent problem are

$$\theta(z = 0) = C, \quad U(z = 0) = V(z = 0) = 0. \quad (5)$$

As in the traditional Prandtl model with $f = 0$, we now attempt to derive a steady solution. After dropping the time derivatives in Equations (1)–(3), one may obtain identical sixth-order partial differential equations for each of the unknowns. Letting F represent either θ , U or V this governing equation is

$$\frac{\partial^2}{\partial z^2} \left(\frac{\partial^4 F}{\partial z^4} + \sigma^4 F \right) = 0, \quad (6)$$

where

$$\sigma^4 = \frac{N^2 \text{Pr} \sin^2(\alpha)}{K^2 \text{Pr}^2} (1 + \Delta), \quad \Delta = \frac{f^2 \cot^2(\alpha)}{N^2 \text{Pr}} \quad (7)$$

Here N is the buoyancy (Brunt–Vaisala) frequency, satisfying $N^2 = \gamma g / \theta_0$. An upper boundary condition is required to complete the solution of Equation (6). Although it is clear that at any finite time $F(z \rightarrow \infty) = 0$, it is less obvious how to specify the upper boundary condition to reflect correctly the solution to the initial-value problem (1)–(3) in the limit $t \rightarrow \infty$. For the moment we simply require that the steady-state solutions remain bounded as $z \rightarrow \infty$.

In the classical Prandtl model, without the Coriolis force, the equivalent of (6) is

$$\frac{d^4 F}{dz^4} + \sigma^4 F = 0, \tag{8}$$

where F now represents either U or θ , and σ is defined by Equation (7) with $\Delta = 0$. Solutions to (8), e.g. Egger (1990) or Grisogono and Oerlemans (2001), are

$$\theta_s = C e^{-z/h_p} \cos(z/h_p), \tag{9}$$

$$U_s = \frac{CK\sigma^2}{\gamma \sin(\alpha)} e^{-z/h_p} \sin(z/h_p), \tag{10}$$

where the Prandtl layer height is $h_p = \sqrt{2}/\sigma$.

The solutions to (6) include functions of the form (9) and (10), satisfying the classical $f = 0$ problem (8), as well as possible functions of the form $az + b$. Since the solution must remain bounded as $z \rightarrow \infty$, a must be zero. Unlike in the classical Prandtl model, it is not possible to obtain a solution to (6) satisfying the lower boundary conditions (4) with all b set to zero. Letting $\tilde{C} = C/(1 + \Delta)$, the solution to (6) subject to the BC (5) that remains bounded as $z \rightarrow \infty$ is

$$\theta_{fs} = \tilde{C} \{ e^{-z/h_p} \cos(z/h_p) + \Delta \}, \tag{11}$$

$$U_{fs} = \frac{\tilde{C}K\sigma^2}{\gamma \sin(\alpha)} e^{-z/h_p} \sin(z/h_p), \tag{12}$$

$$V_{fs} = \frac{\tilde{C} f \cot(\alpha)}{\text{Pr} \gamma} \{ e^{-z/h_p} \cos(z/h_p) - 1 \}. \tag{13}$$

This solution has the counter-intuitive property that neither θ_{fs} nor V_{fs} approaches zero as $z \rightarrow \infty$; however

as will be demonstrated, at any *finite* z , (11)–(13) do give the solutions to the initial-value problem (1)–(3) in the limit $t \rightarrow \infty$.

3. Asymptotic time-dependent model and numerical results

Observe that U and θ are coupled to V solely by the Coriolis term in the down-slope momentum equation. For small-slope angles, the ratio of this Coriolis term to the buoyancy term in (1) is approximately $Vf\theta_0/\alpha g\theta$. For typical katabatic flows, characteristic scales for these parameters are $\alpha = 5^\circ \sim 0.1$ radians, $\theta/\theta_0 \sim 0.01$, and $V \sim 1 \text{ m s}^{-1}$, implying that $Vf\theta_0/\alpha g\theta \sim O(10^{-2})$ and that reasonable approximations to U and θ can be obtained with the Coriolis term neglected in (1). Since (1) and (3) become decoupled from (2) when the Coriolis term is neglected in (1), the approximate solutions for the steady-state potential temperature perturbation and down-slope velocity component are the same as in the classical Prandtl model: (9) and (10), with σ computed by setting $\Delta = 0$ in (7).

Further confirmation that the classical Prandtl-model solutions remain good approximations to the actual steady-state solution even when Coriolis forces are present may be obtained by noting that they approach U_{fs} and θ_{fs} as $\Delta \rightarrow 0$. For a typical katabatic flow, $\alpha \sim 0.1$ radians, $N \sim 0.01 \text{ s}^{-1}$ and $\text{Pr} \sim 1$, so Δ is $O(10^{-2})$ and U_s and θ_s closely approximate U_{fs} and θ_{fs} .

Before attempting to determine an approximate analytic expression for the cross-slope velocity that is relevant on appropriate atmospheric time-scales, let us investigate numerical solutions of the time-dependent system (1)–(3). This system will be integrated past the time when U and θ become quasi-steady, but terminated before the

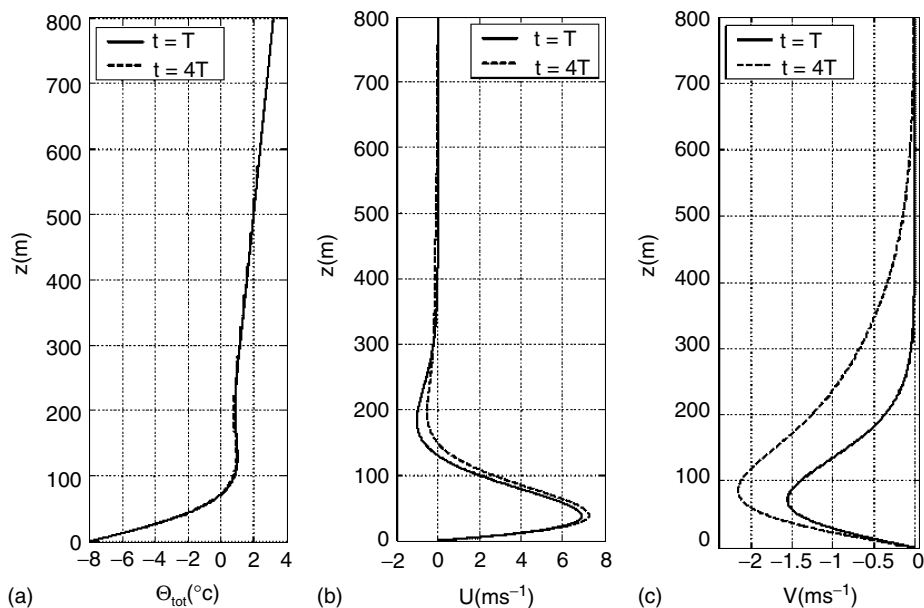


Figure 1. Numerical solution for the Prandtl model (a) $\theta_{\text{tot}} = \theta + \gamma z$, (b) U and (c) V . Here $f = 1.1 \times 10^{-4} \text{ s}^{-1}$; other parameters are $(\alpha, \gamma, K, \text{Pr}, C) = (-4^\circ, 4 \times 10^{-3} \text{ K m}^{-1}, 1 \text{ m}^2 \text{ s}^{-1}, 1.1, -8 \text{ K})$. Solutions are displayed at $t = T = 2.1 \text{ h}$ (solid) and $t = 4T$ (dashed). The numerical model top is at 2000 m.

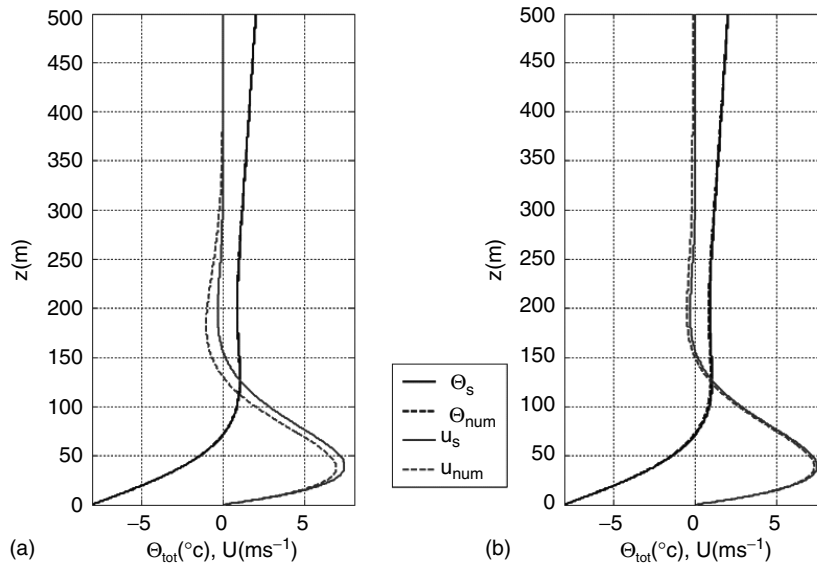


Figure 2. Numerical θ_{num} and U_{num} (dashed) and approximate θ_s and U_s (solid) steady solutions (9) and (10) for the Prandtl model, at (a) $t = T$ and (b) $t = 4T$. The rest as in Figure 1.

solution loses its geophysical relevance or violates the Boussinesq approximation. For instance, the total downslope vertical displacements should be much smaller than the characteristic depth of the troposphere. For slope angles $1\text{--}6^\circ$ and mean katabatic wind speeds $2\text{--}5\text{ m s}^{-1}$, the flow takes between 1 and 7 h to become steady, i.e. less than the duration of an inertial oscillation.

In the non-rotating case, U and θ asymptotically approach their steady-state values after the time $T = 2\pi/\{N \sin(\alpha)\}$ (Grisogono, 2003). Figure 1 shows the structure of the flow in the rotating case at times T and $4T$, obtained using the numerical model from Grisogono (2003) for a case with physical parameters $(f, \alpha, \gamma, K, \text{Pr}, C) = (1.1 \cdot 10^{-4} \text{ s}^{-1}, -4^\circ, 4 \cdot 10^{-3} \text{ K m}^{-1}, 1 \text{ m}^2 \text{ s}^{-1}, 1.1, -8 \text{ K})$. Note that U and θ are almost steady after time T , but that V continues to increase through a several-hundred-metre-thick layer. Nevertheless, changes in V do not exert a significant influence on U and θ , which as shown in Figure 2 remain very close to the steady functions U_s and θ_s from (9) and (10) with $\Delta = 0$ in the expression for σ . This is in accord with the preceding scale analysis. Also, idealized 48 h simulations of katabatic flow down a topographic cross-section representative of Coats Land, Antarctica (Renfrew, 2004) show the depth of the cross-slope velocity increasing with time while the height and structure of the downslope jet remains constant in a manner qualitatively similar to that shown in Figure 1(b) and (c). A more detailed comparison of our results and those of Renfrew (2004) is hindered by the differences in the simulations: the topography considered by Renfrew is not a uniform constant slope and the mixing is primarily produced by a non-uniform eddy diffusion.

For $t > T$, the preceding scale analysis together with the numerical simulations show that U_s and θ_s are good

approximations to U and θ . Thus for $t > T$, the cross-slope momentum equation (2) may be approximated as

$$\frac{\partial V_f}{\partial t} - K \text{Pr} \frac{\partial^2 V_f}{\partial z^2} = -f U_s \cos(\alpha), \quad t > T \quad (14)$$

Here V_f is the approximate time-dependent cross-slope velocity. The solution to (14) subject to the bottom BC (5) is

$$V_f = \frac{C f \cot(\alpha)}{\text{Pr} \gamma} \left\{ e^{-z/h_p} \cos(z/h_p) - 1 + \text{erf}(z/\sqrt{\tau K \text{Pr}}) \right\}. \quad (15)$$

where erf is the error function and $\tau = t - T$. Since $\text{erf}(\infty) = 1$, for any fixed finite time t_0 , $V_f(z, t_0) \rightarrow 0$ as $z \rightarrow \infty$, that is, the V_f perturbations cannot extend to infinite heights in a finite time. Also, since $\text{erf}(0) = 0$, as $t \rightarrow \infty$ at any fixed finite z_0 , $V_f(z_0, t)$ approaches $V_{fs}(z_0, t)$ except for small relative errors proportional to Δ .

As shown in Figure 3, V_f provides an excellent approximation to the time-dependent solution for $t > T$. Turbulent mixing slowly diffuses the katabatically forced V upward from the boundary layer to progressively higher levels, so that V never achieves a true steady state. For most atmospheric applications, (9), (10), and (15) provide good approximations from which one can easily obtain turbulent fluxes. Nevertheless, for a given time-scale of interest, one can still attempt to find asymptotic steady solutions (Stiperski *et al.*, 2005).

4. Conclusion

Probably the best model for studying simple katabatic flows is that of Prandtl. Hence, the Prandtl model is a

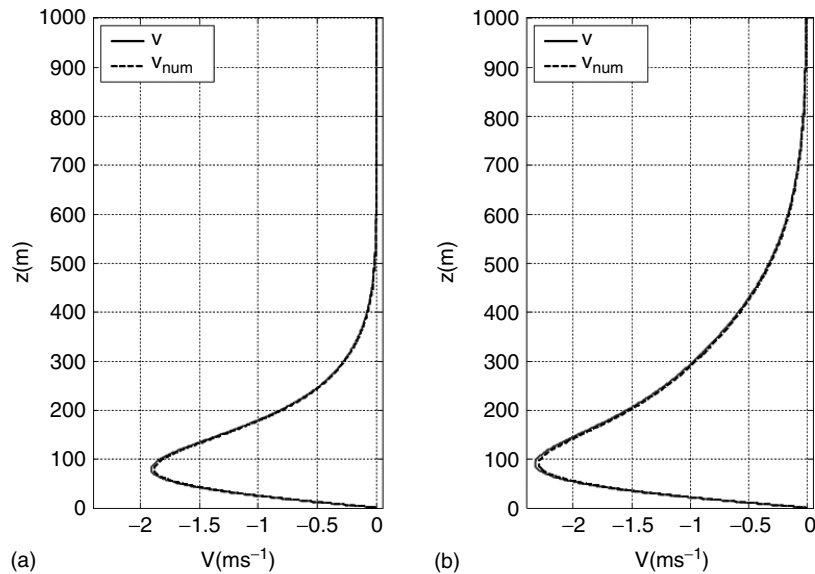


Figure 3. Numerical V_{num} (dashed) and time-dependent asymptotic V_f (solid) solutions obtained from (15) for (a) $t = 2T$ and (b) $t = 6T$. The physical parameters governing this problem are the same as in Figure 1.

tempting way of treating long cool (sub)polar slopes that generate katabatic flows in the long-lived strongly-stable ABL. It is shown that the steady Prandtl model including the Coriolis force, $f \neq 0$, is not equivalent to its time-dependent counterpart, even after long time periods. This is an important issue for parameterizations, which often assume the existence of a steady state.

We calculate the flow vector $F = (\theta, U, V)$ numerically and analytically. While U and θ reach their steady-state profiles after the typical time-scale for simple katabatic flows $T \approx 2\pi/\{N \sin(\alpha)\}$, V diffuses upwards in time without a well-defined time-scale. Moreover, Equation (15) indicates that V may affect the circum-polar stratospheric vortex after a few months of polar night. Solving a more complete system would demonstrate more clearly the relationship between the vortex and the katabatic flow suggested by van den Broeke and van Lipzig (2003).

The simplest Prandtl model with the Coriolis effect should therefore include time-variations of the cross-slope wind component. The proposed analytic solutions, (9), (10) and (15), can be used for studying katabatic flows over long slopes, especially for surface flux parameterizations in climate models and data analysis.

Acknowledgements

We thank Stephen Griffiths for his insightful comments and an anonymous reviewer for directing us to the work of I. A. Renfrew. Another reviewer indirectly inspired the inclusion of the Appendix, and we are grateful for this.

This study was supported by the Croatian Ministry of Science under the projects 004-1193086-3036 (Meteorological and Hydrological Service), 0037114 (Dept of Mathematics) and 0119339 and BORA (Dept of Geophysics). DRD’s research was supported by NSF grant ATM-0506589.

Appendix

Equations (1)–(3) are obtained by transforming the Boussinesq momentum, and thermodynamic equations to the sloping (x, y, z) coordinate system using the relationships

$$\begin{aligned} X &= x \cos(\alpha) - z \sin(\alpha), & Y &= y, \\ Z &= x \sin(\alpha) + z \cos(\alpha), \\ u &= U \cos(\alpha) - W \sin(\alpha), & v &= V, \\ w &= U \sin(\alpha) + W \cos(\alpha) \end{aligned}$$

and

$$\begin{aligned} \frac{\partial}{\partial X} &= \frac{\partial x}{\partial X} \frac{\partial}{\partial x} + \frac{\partial z}{\partial X} \frac{\partial}{\partial z} = \cos(\alpha) \frac{\partial}{\partial x} - \sin(\alpha) \frac{\partial}{\partial z}, \\ \frac{\partial}{\partial Z} &= \frac{\partial x}{\partial Z} \frac{\partial}{\partial x} + \frac{\partial z}{\partial Z} \frac{\partial}{\partial z} = \sin(\alpha) \frac{\partial}{\partial x} + \cos(\alpha) \frac{\partial}{\partial z}, \end{aligned}$$

where (X, Y, Z) and (u, v, w) are the coordinates and velocities in the standard un-rotated system. It should be emphasized that (1)–(3) apply only in the special case where W and the partial derivatives with respect to x and y are all zero. To derive (1), let P be the Boussinesq pressure. Then the transformed x -momentum equation is

$$\frac{\partial U}{\partial t} \cos(\alpha) - \sin(\alpha) \frac{\partial P}{\partial z} = fV + K \text{Pr} \frac{\partial^2 U}{\partial z^2} \cos(\alpha), \tag{A.1}$$

and the vertical momentum equation becomes

$$\frac{\partial U}{\partial t} \sin(\alpha) + \cos(\alpha) \frac{\partial P}{\partial z} = g \frac{\theta}{\theta_0} + K \text{Pr} \frac{\partial^2 U}{\partial z^2} \sin(\alpha). \tag{A.2}$$

Equation (1) is formed by multiplying (A.1) times $\cos(\alpha)$ and adding the result to (A.2) times $\sin(\alpha)$.

To appreciate the differences between (A.1) – (A.2) and the corresponding results for flows with more general spatial dependence, consider the equations linearized about a resting basic state, but do not assume that $W = 0$ or that the solutions are independent of x and y . Then the x -momentum equation transforms to

$$\begin{aligned} \frac{\partial}{\partial t} \{U \cos(\alpha) - W \sin(\alpha)\} + \cos(\alpha) \frac{\partial P}{\partial x} \\ - \sin(\alpha) \frac{\partial P}{\partial z} = fV + K \text{Pr} \nabla^2 \{U \cos(\alpha) - W \sin(\alpha)\}, \end{aligned} \quad (\text{A.3})$$

and the transformed vertical momentum equation becomes

$$\begin{aligned} \frac{\partial}{\partial t} \{U \sin(\alpha) + W \cos(\alpha)\} + \sin(\alpha) \frac{\partial P}{\partial x} + \cos(\alpha) \frac{\partial P}{\partial z} \\ = g \frac{\theta}{\theta_0} + K \text{Pr} \nabla^2 \{U \sin(\alpha) + W \cos(\alpha)\}. \end{aligned} \quad (\text{A.4})$$

Momentum equations along the x and z coordinates similar to those given by previous authors (Mahrt, 1982), may now be obtained. Multiplying (A.3) by $\cos(\alpha)$ and adding $-\sin(\alpha)$ times (A.4) yields

$$\frac{\partial U}{\partial t} + \frac{\partial P}{\partial x} = fV \cos(\alpha) + g \frac{\theta}{\theta_0} \sin(\alpha) + K \text{Pr} \nabla^2 U. \quad (\text{A.5})$$

Similar manipulations give the linearized momentum equation along the coordinate perpendicular to the surface

$$\frac{\partial W}{\partial t} + \frac{\partial P}{\partial z} = -fV \sin(\alpha) + g \frac{\theta}{\theta_0} \cos(\alpha) + K \text{Pr} \nabla^2 W. \quad (\text{A.6})$$

If non-linear advection had been included, $(\mathbf{V} \cdot \nabla)U$ would appear on the left hand side of (A.5) and $(\mathbf{V} \cdot \nabla)W$ would be included in (A.6).

References

- Conangla L, Cuxart J. 2006. On the turbulence in the upper part of the low-level jet: an experimental and numerical study. *Boundary-Layer Meteorol.* **118**: 379–400.
- Denby B. 1999. Second-order modelling of turbulence in katabatic flows. *Boundary-Layer Meteorol.* **92**: 65–98.
- Denby B, Greuell W, Oerlemans J. 2002. Simulating the Greenland atmospheric boundary layer. Part II: Energy balance and climate sensitivity. *Tellus* **54A**: 539–541.
- Derbyshire SH. 1999. Boundary layer decoupling over cold surfaces as a physical boundary instability. *Boundary-Layer Meteorol.* **90**: 297–325.
- Egger J. 1990. Thermally forced flows: theory. In *Atmospheric Processes over Complex Terrain*, Meteorol. Monogr. Amer. Meteorol. Soc.: No 45: 43–57.
- Grisogono B. 2003. Post-onset behaviour of the pure katabatic flow. *Boundary-Layer Meteorol.* **107**: 157–175.
- Grisogono B, Oerlemans J. 2001. A theory for the estimation of surface fluxes in simple katabatic flows. *Q. J. R. Meteorol. Soc.* **127**: 2725–2739.
- Grisogono B, Oerlemans J. 2002. Justifying the WKB approximation in the pure katabatic flows. *Tellus* **54A**: 453–462.
- Heinemann G, Klein, T. 2002. Modelling and observations of the katabatic flow dynamics over Greenland. *Tellus* **54A**: 542–554.
- Mahrt L. 1982. Momentum balance of gravity flows. *J. Atmos. Sci.* **39**: 2701–2711.
- Parmhed O, Oerlemans J, Grisogono B. 2004. Describing the surface fluxes in the katabatic flow on Breidamerkurjokull, Iceland. *Q. J. R. Meteorol. Soc.* **130**: 1137–1151.
- Renfrew IA. 2004. The dynamics of idealized katabatic flow over a moderate slope and ice shelf. *Q. J. R. Meteorol. Soc.* **130**: 1023–1045.
- Stiperski I, Kavčič I, Grisogono B. 2005. Katabatic flow with coriolis effect. *Cro. Meteorol. J.* **40**: 470–473.
- Van den Broeke MR, van Lipzig NPM, van Meijgaard E. 2002. Momentum budget of the east-Antarctic atmospheric boundary layer: results of a regional climate model. *J. Atmos. Sci.* **59**: 3117–3129.
- Van den Broeke MR, van Lipzig NPM. 2003. Factors controlling the near-surface wind field in Antarctica. *Mon. Weather Rev.* **131**: 733–743.